# Position Sensing Fault Detection and Compensation of BLDC Motors Based on Fault Index Functions

Taehyung Kim
Electrical and Computer Engineering
University of Michigan-Dearborn
Dearborn, MI, 48128 USA
taehyung@umich.edu

Sahithya Parvathareddy

Electrical and Computer Engineering

University of Michigan-Dearborn

Dearborn, MI, 48128 USA

sahip@umich.edu

Anuj Shah

Electrical and Computer Engineering
University of Michigan-Dearborn
Dearborn, MI, 48128 USA
sanuj@umich.edu

Abstract— BLDC motors are widely employed in various applications because of their high efficiency, reliability, and long operational life. For BLDC motors, any electric malfunctions in the commutation signal creation with or without Hall sensors can lead to unexpected vibrations, crashes, and accidents according to application areas. Therefore, fast detection and diagnosis of these faults are crucial for the reliable operation of BLDC motor drive systems. In this paper, a unique approach has been explored for developing fault signatures to detect commutation signal faults accurately and rapidly in the BLDC motor drive system under highly dynamic loads. After the fault detection, a commutation signal is indirectly reconstructed based on healthy commutation signals to continuously drive the motor drive system to avoid serious electrical and mechanical issues due to the faults. The proposed approach and feasibility of the method have been verified both by simulation and experimental studies. The results of the proposed method will significantly improve the accuracy of the commutation signal fault detection and eventually enhance the reliability of the BLDC motor drive.

Keywords— BLDC motor, Position Sensor, Fault

## I. INTRODUCTION

BLDC motors are increasingly being utilized for numerous industrial and commercial applications, including transportation systems, home appliances, electric tools, industrial automation systems, etc. The cost-effective drive system with a simpler control structure without requiring expensive position sensors is the main attraction, on top of the decent efficiency and performance. The decreasing controller costs with cost-effective DSPs have paved the way to extend the application areas of the BLDC motors. More electric vehicles, trains, ships, and aircraft are the newer application areas of the motor, and recent advancements in robots and small aircraft such as drones have expanded the use of BLDC motors.

In this paper, among the various application areas of BLDC motors, several crucial areas that are directly related to safety, such as UAVs (unmanned aerial vehicles) and electric steering systems in electrified vehicles, are mainly targeted. For UAVs and drones, outer rotor-type BLDC motors are commonly used (as shown in Fig. 1(a)).

This work was supported by the National Science Foundation grant, award no. 2321681, and the RID UM-Dearborn grant, no. U087256.

On the other hand, inner rotor-type motors are typically used for electrified vehicles (as exemplified in Fig. 1(b)). The BLDC drive systems are widely employed due to their decent efficiency, lower cost, simple control, and easy maintenance [1]-[3].

The fundamental operational principles of BLDC motor drive systems are basically the same as those of traditional permanent magnet motor drive systems. However, in order to achieve optimal performance from the BLDC motors, the square-shaped state current should be properly synchronized with the induced back-EMF (electro motive force) voltage. It is essential to note that, due to the trapezoidal shape of the induced EMF (back-EMF) in motor phase windings, a square-shape current waveform would result in a maximum torque density for the BLDC motor [1].

The typical BLDC motor has a permanent magnet rotor and stator windings with current-flowing conductors. Compared to a permanent magnet DC motor, the BLDC motor has an inverted operational structure without mechanical brushes or commutators. The DC machine requires mechanical commutators to reverse the current direction to produce unidirectional torque. The BLDC motors rely on power switches and position sensors for electronic current communications. When the rotor's permanent magnets pass by the stator winding, current needs commutation using Hall-effect position sensors or position sensorless commutation logics. Hall-effect position sensors and sensorless drive structures are usually cost-effective solutions, and hence the probability of malfunction is not low.

The 120° current-driven BLDC motor drive requires only six commutation points in one revolution, and hence the control structure is much simpler than a 180° sinewave drive system. Any malfunction in the Hall position sensors or in the sensorless position detection circuitry can cause serious performance problems or complete stoppage of the drive system. To avoid these downfalls, the malfunction in the commutation point detection needs to be promptly detected, and a proper remedial action should be taken to continue the motor drive operation, especially for safety-related applications.

In [4], three Hall sensor signals are modified to a two-axis frame ( $\alpha$  and  $\beta$ ), and the zero vector is utilized based on a look-up table to detect sensor faults. A rotary vector is used in [5] based on the observation that the BLDC motor operates only in

four sectors if a sensor fails. In [6], simple combinatory functions based on three binary numbers are used to detect Hall sensor faults. In addition, [7] employs PWM input capture functions to diagnose Hall sensor faults for 180° sinewave drives.

In this paper, a new method based on three fault index functions to detect commutation faults (either by Hall sensor or by sensorless drive) for 120° current drive for BLDC motors has been investigated, along with a remedial approach for continuous drive, especially for safety-related applications. The detection method is simplified to apply the approach to wider application areas, including high-speed motor drive systems. In addition, the utilization of three fault index functions can improve detection accuracy with faster decision-making, especially for highly dynamic load applications. The proposed concept and feasibility have been verified both by simulations and experiments.

# II. PROPOSED APPROACH

The BLDC motor and its electronic speed controller (ESC) for small aircraft are exemplified in Fig. 1(a). A typical BLDC motor stator has a 3-phase full-pitch, concentrated winding arrangement that generates a trapezoid-shaped phase back-EMF waveform as shown in Fig. 1(c) [2], [8]-[10]. The BLDC motor has a phase-to-neutral point voltage equation (phase A is exemplified) as follows:

$$\begin{split} V_{an} &= R_a i_a + L_{aa} \frac{di_a}{dt} + L_{ab} \frac{di_b}{dt} + L_{ac} \frac{di_c}{dt} + \\ & \pi^2(Dl) f \sum_{k=1}^{\infty} N_a B_k \cdot cos(k(\theta_e)) \end{split} \tag{1}$$

where  $R_a$ , f, D, l,  $\theta_e$ ,  $N_a$ ,  $L_{aa}$ ,  $L_{ab}$ , and  $B_k$  denote phase A resistance, frequency, stator diameter, motor length, electrical angle, phase A number of turns, phase A self-inductance, mutual inductance between phases A and B, and flux density, respectively. The last term in (1) formulates a phase back-EMF, which is a trapezoid waveform as shown in Fig. 1 (c). Ideally, with the trapezoid back-EMF, a 120° rectangular current can produce constant torque with the flat portion of the back-EMF shape

For BLDC motors, the back-EMF is formulated by the stator flux linkage,  $\lambda_s$ .

$$\lambda_{s} = (\pi r l) B_{f} (\theta / (\pi/2)) \qquad (-\pi/2 \le \theta \le \pi/2) \quad (2)$$

Where,  $\theta$ ,  $B_f$ , and l are position, flux density, and motor length, respectively. The derivative of the flux linkage will produce the motor back-EMF (for a single turn coil) as:

$$e_s = \frac{d\lambda_s}{dt} = \frac{d\lambda_s}{d\theta} \cdot \frac{d\theta}{dt} = \frac{\pi r l B_f \omega_r}{\pi/2} = 2B_f l r \omega_r$$
 (3)

The back-EMF magnitude considering the total number of turns of each phase winding  $(N_S)$  will be:

$$E = 2N_S B_f lr \omega_r \tag{4}$$

The phase voltage equation is formulated by adding the winding resistance's voltage drop, inductor voltage, and phase back-EMF as (5).

$$\begin{bmatrix} v_a \\ v_b \\ v_c \end{bmatrix} = \begin{bmatrix} R & 0 & 0 \\ 0 & R & 0 \\ 0 & 0 & R \end{bmatrix} \begin{bmatrix} i_a \\ i_b \\ i_c \end{bmatrix} + \begin{bmatrix} L & 0 & 0 \\ 0 & L & 0 \\ 0 & 0 & L \end{bmatrix} \frac{d}{dt} \begin{bmatrix} i_a \\ i_b \\ i_c \end{bmatrix} + \begin{bmatrix} e_a \\ e_b \\ e_c \end{bmatrix}$$
(5)

$$L = L_{\rm S} - L_{\rm M} \tag{6}$$

Where,  $v_a$ , R,  $i_a$ ,  $e_a$ ,  $L_s$ , and  $L_M$  stand for phase A voltage, phase winding resistance, phase A current, back-EMF, self, and mutual inductances, respectively. The total motor torque is produced from the back-EMFs, stator currents, and rotor speed as follows:

$$T_{tot} = \frac{i_a e_a + i_b e_b + i_c e_c}{\omega} \tag{7}$$

Where,  $\omega$ ,  $e_a$ , and  $i_a$  denote the rotor speed, phase A back-EMF, and phase A current, respectively. From (7), it can be seen that in order to produce constant torque for BLDC motors, each excited phase should be synchronized with the flat portion of the back-EMF, as shown in Fig. 1(c).

The BLDC motors have two ways to commutate currents for the 120° conduction drive. Employing Hall effect position sensors is an easy way to directly detect the rotor position and create commutation instants for a BLDC motor. However, due to the cost of the position sensors and reliability issues in hot and harsh operating conditions, position sensorless drives have been used for various applications [3].

Fig. 2 presents a typical BLDC motor drive system configuration with speed and current regulation capabilities. For current commutation, the drive accepts position feedback from position sensors (Hall effect type), and the shaft speed is calculated based on the sensing signals for the speed control loop. For electric propulsion applications, an electronic speed controller (ESC) is widely used. The ESC for BLDC motors that is typically in small aircraft and vehicles includes circuits to detect commutation points without Hall effect position sensors based on circuits exemplified in Fig. 3(a) [11].



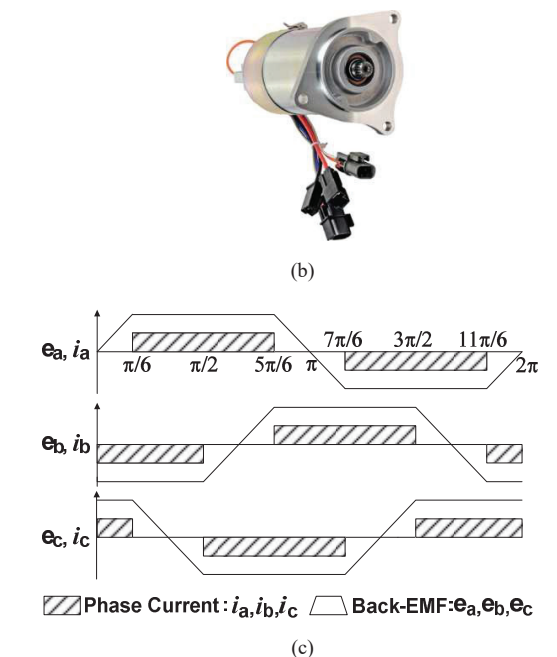


Fig. 1. BLDC motor drive system, (a) BLDC motor and electronic speed controller (ESC) for UAVs; (b) BLDC motor for an electric power steering system; (c) Ideal back-EMF and current waveforms.

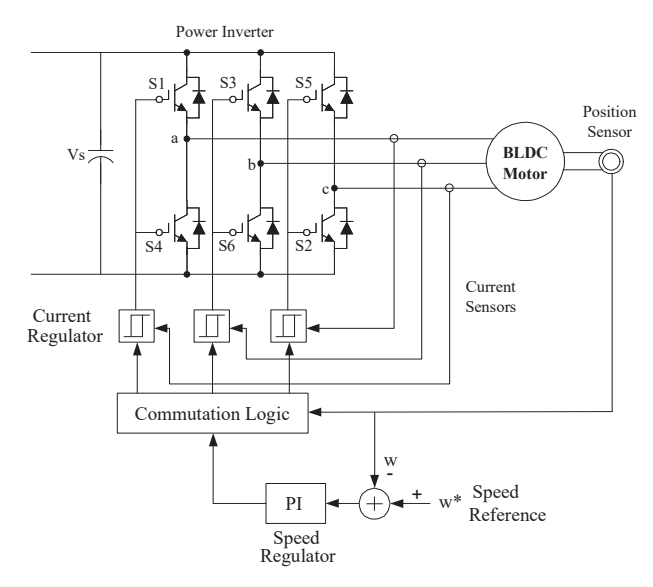
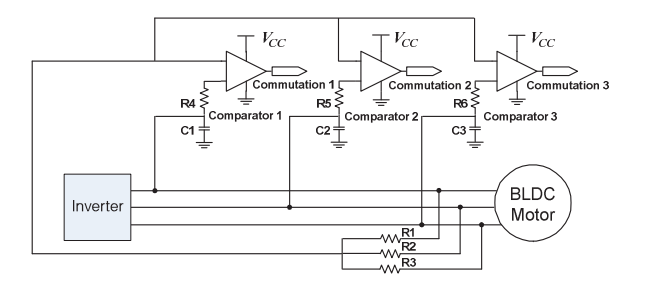


Fig. 2. Typical BLDC motor drive configuration with speed and current control loops.

Therefore, the commutation signals can be created with or without position sensors depending on the product, and Fig. 3(b) presents the typical commutation signals created by sensors or sensorless detection circuits to drive a BLDC motor. The commutation signal can malfunction due to a sensor failure (for a drive with position sensors) or a fault in the sensorless detection circuitry (for a sensorless drive as shown in Fig. 3(a)). To detect the commutation signal fault, three-phase fault index functions are formulated.



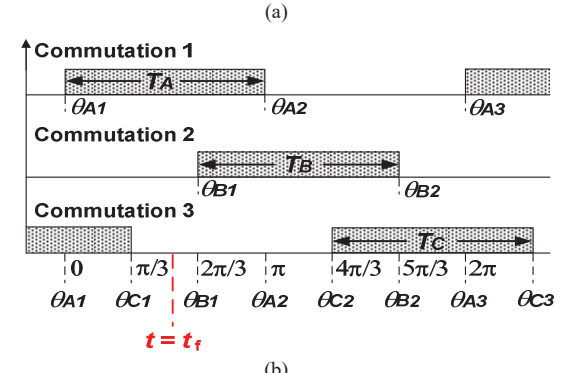


Fig. 3. (a) Typical sensorless position detection circuits in ESCs. (b) commutation signals for BLDC motor drive systems.

$$\Gamma_{A\_index} = \frac{\sqrt[\pi]{\sum_{k=0}^{N_A} \xi_{is}}}{\sqrt[\frac{1}{2} \left( \sqrt[\pi]{\sum_{m=0}^{N_B} \xi_{is}} + \sqrt[\pi]{\sum_{n=0}^{N_C} \xi_{is}} \right)}}$$
(8)

$$\Gamma_{B\_index} = \frac{\sqrt[\pi]{\sum_{m=0}^{N_B} \xi_{is}}}{\frac{1}{2} \left( \sqrt[\pi]{\sum_{k=0}^{N_A} \xi_{is}} + \sqrt[\pi]{\sum_{n=0}^{N_C} \xi_{is}} \right)}$$
(9)

$$\Gamma_{C\_index} = \frac{\pi / \sum_{n=0}^{N_C} \xi_{is}}{\frac{1}{2} (\pi / \sum_{k=0}^{N_A} \xi_{is}^{+ \pi} / \sum_{m=0}^{N_B} \xi_{is})}$$
(10)

Where,  $\xi_{is}$  is the period of each timer interrupt service routine of a microprocessor, and  $N_A$ ,  $N_B$ , and  $N_C$  are the timer counter numbers increased from zero until the commutation signal toggles. Once a commutation signal fault occurs (assuming the phase A commutation signal fault), the counter k for phase A (m for phase B and m for phase C) will keep on increasing right after the fault. Therefore,  $\Gamma_{A\_index}$  will increase significantly while  $\Gamma_{B\_index}$  and  $\Gamma_{C\_index}$  decrease. Based on a predetermined threshold value,  $F_{th}$ , considering a normal maximum load change and acceleration, the commutation signal fault can be detected. If a phase A commutation signal fault is detected, the commutation instants for phase A commutation can be estimated based on Fig. 3(b) as

$$\widetilde{\theta_{A2}} = \int_0^{t_1} \frac{\pi}{T_C(k-1)} \cdot dt + \theta_{B1} = \pi$$
 (11)

$$\widetilde{\theta_{A3}} = \int_0^{t_2} \frac{\pi}{T_B(k)} \cdot dt + \theta_{B2} = 2\pi$$
 (12)

The moments  $t_1$  and  $t_2$  are determined when the estimated commutation angles,  $\widetilde{\theta_{A2}}$  and  $\widetilde{\theta_{A3}}$ , reach  $\pi$  and  $2\pi$ , respectively.  $T_C(k-1)$  and  $T_B(k)$  are the previous and current time durations of the phase C and B commutation signals (time duration between rising and falling edges of the commutation signals). Figure 4(a) indicates the simulation results of a BLDC motor drive response, assuming that phase A commutation signal generation failed at t=1 sec.

Due to the commutation signal fault, a large speed ripple occurs. Figure 4(b) presents the drive response of the commutation signal fault detection and compensation. It is assumed that a commutation signal fault (from phase A) occurred at t = 0.6 sec, and fault detection based on (8)-(10) and compensation by (11) and (12) are applied to recreate commutation signals for phase A. In addition, Figs. 5 and 6 present experimental results under the commutation signal fault in the phase A commutation signal.

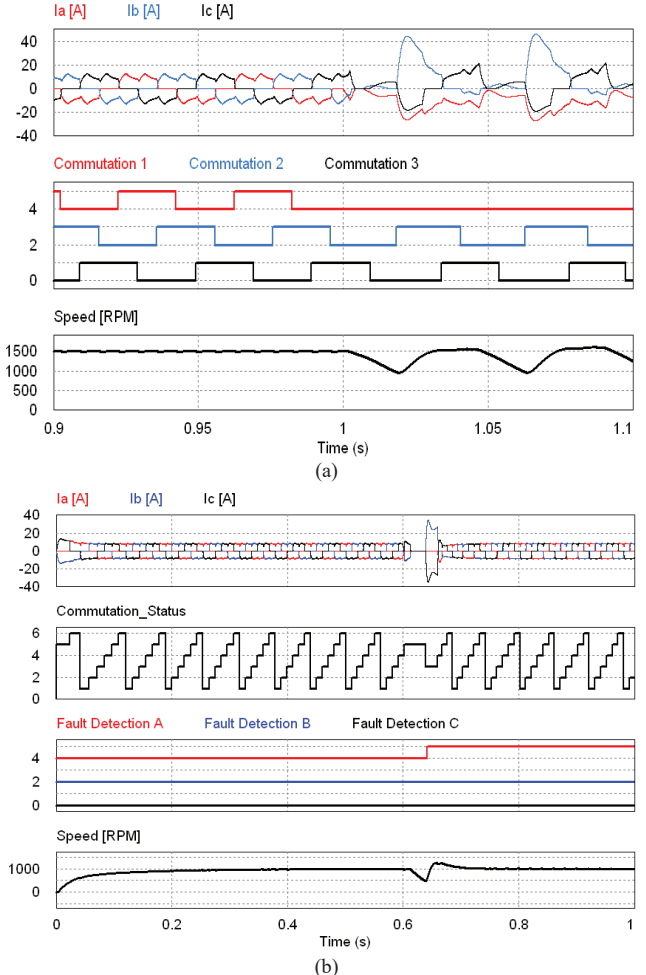


Fig. 4. Simulation results. (a) BLDC drive response under a commutation signal fault (assumed phase A fault at t = 1 sec); (b) BLDC drive response based on the proposed commutation signal fault detection and compensation methods.

Fig. 5 presents the drive response under the fault without any remedial actions. The commutation signal A is logic zero after

the fault occurs and unbalanced current flows, causing a significant speed ripple. On the other hand, Fig. 6 shows the drive response after the fault with the proposed detection and compensation methods. The commutation status signal (bottom waveform of Fig. 6(a)) indicates the commutation fault that occurred and the response after fault detection and remedial action. The fault detection approach based on (8)-(10) identifies the commutation fault, and the remedial approach based on (11)-(12) immediately applied to reconstruct the commutation instants.

As shown in the phase A current waveform of Fig. 6(a), the phase current shape is back to normal after the proposed detection by fault index functions and the remedial approach. Fig. 6(b) presents a different phase current (phase B) and speed response. The motor speed initially decreases right after the fault occurrence. After the remedial action, the motor speed goes back to a normal steady-state speed after a short perturbation period. The simulation and experimental results indicate that this type of commutation signal fault can be compensated based on the proposed approach. Through simulation studies as shown in Fig. 4 and experimental results in Figs. 5 and 6, the feasibility of the fault index functions and the effectiveness of the compensation method by (11)-(12) have been successfully verified. The proposed approaches can be applied to various industrial and commercial applications that require reliability and continuous drive even under commutation signal faults.

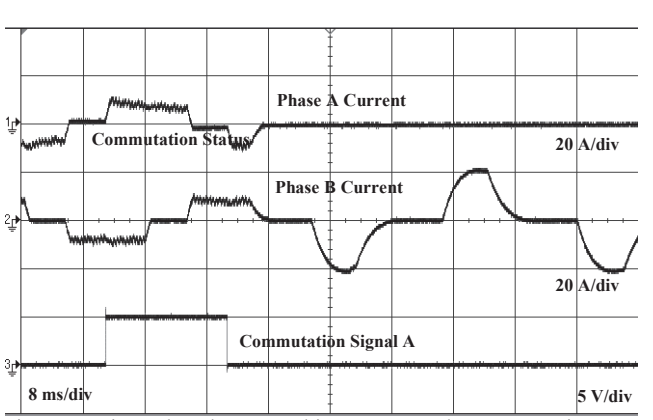
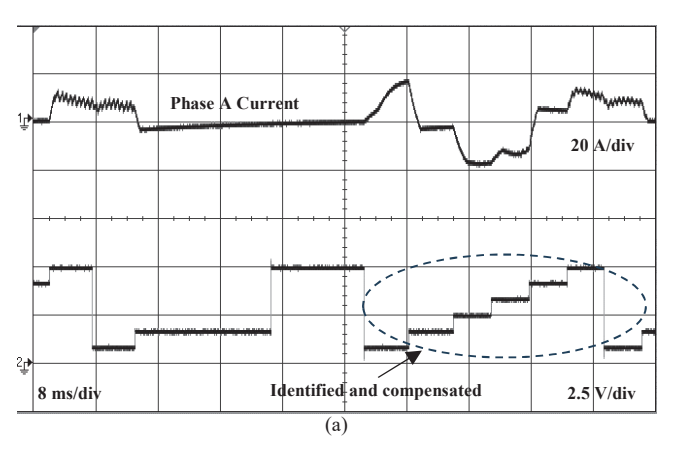


Fig. 5. Experimental results: BLDC drive response under a commutation signal fault (no remedial action was taken).



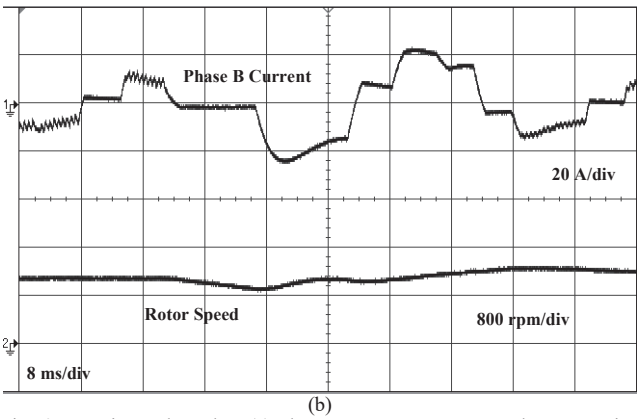


Fig. 6. Experimental result: ; (a) Phase A current response and commutation status with proposed fault detection and remedial approaches (b) Phase B current and speed responses with the proposed fault detection and remedial approaches.

### III. CONCLUSIONS

In this paper, a new approach to detecting communication signal faults in a three-phase BLDC motor control system with 120° current conduction is presented. The proposed detection method is based on three fault index functions, which are not computationally intensive and less sensitive to load changes, to avoid false alarms. A remedial commutation construction has also been investigated based on the remaining healthy commutation signals. The fault compensation method can effectively create commutation signals to continuously drive the BLDC motor without fatal consequences. The proposed concepts and feasibility of the fault detection and remedial approaches were verified both by simulation and experimental studies.

### ACKNOWLEDGMENT

This work was supported by the National Science Foundation grant, award no. 2321681, and the RID UM-Dearborn grant, no. U087256.

### REFERENCES

- [1] J. R. Hendershot Jr. and T. J. E. Miller, Design of brushless permanent-magnet motors. *Oxford Magna Physics Publications*, ISBN 1-881855-03-1, 1994.
- [2] Gong, A., MacNeill, R., and Verstraete, D., "Performance Testing and Modeling of a Brushless DC Motor, Electronic Speed Controller and Propeller for a Small UAV Application," 54th AIAA/SAE/ASEE Joint Propulsion Conference, Cincinnati, OH, USA, 2018.
- [3] T. Kim and M. Ehsani, "Sensorless Control of the BLDC Motors From Near Zero to High Speed," IEEE Transactions on Power Electronics, vol. 19, no. 6, pp. 1635-1645, 2004.
- [4] G. Scelba, G. De Donato, G. Scarcella, F. Giulii Capponi, and F. Bonaccorso, "Fault-tolerant rotor position and velocity estimation using binary Hall-effect sensors for low-cost vector control drives," IEEE Trans. Ind. Appl., vol. 50, no. 5, pp. 1629–1636, Sep./Oct. 2014.
- [5] G. Scelba, G. De Donato, M. Pulvirenti, F. Giulii Capponi, and G. Scarcella, "Hall-effect sensor fault detection, identification and compensation in brushless DC drives," IEEE Trans. Ind. Appl., vol. 52, no. 2, pp. 1542–1554, Mar./Apr. 2016.
- [6] Zhang, Y., Wang, H.-C., Wei, H.-F., Li, Y.-J., Li, K.-L. and Liu, W.-T., "New fault-tolerant control method for Hall signals in brushless DC motor driver of E-bicycle," in IET Electron. Lett., vol. 56, no. 6, pp. 284-286, 2020.
- [7] A. Mousmi, A. Abbou and Y. El Houm, "Binary Diagnosis of Hall Effect Sensors in Brushless DC Motor Drives," in IEEE Transactions on Power Electronics, vol. 35, no. 4, pp. 3859-3868, April 2020.
- [8] D. Mohanraj et al., "A Review of BLDC Motor: State of Art, Advanced Control Techniques, and Applications," in IEEE Access, vol. 10, pp. 54833-54869, 2022.
- [9] R. L. Valle, P. M. De Almeida, G. A. Fogli, A. A. Ferreira and P. G. Barbosa, "Simple and Effective Digital Control of a Variable-Speed Low Inductance BLDC Motor Drive," in IEEE Access, vol. 8, pp. 13240-13250, 2020.
- [10] C. Cui, G. Liu and K. Wang, "A Novel Drive Method for High-Speed Brushless DC Motor Operating in a Wide Range," in IEEE Transactions on Power Electronics, vol. 30, no. 9, pp. 4998-5008, Sept. 2015.
- [11] J. Molnar, D. Drabiscak, P. Jacko, M. Guzan and M. Maliakova, "Design of motor speed controller of electronic commutation," 2017 International Conference on Modern Electrical and Energy Systems (MEES), pp. 276-279, Kremenchuk, Ukraine, 2017.